Human Molecular Genetics, 2005, Vol. 14, No. 13 **1863–1876**
doi:10.1093/hmg/ddi192
Advance Access published on May 11, 2005

Gene expression in Huntington's disease skeletal muscle: a potential biomarker

Andrew D. Strand[1,*], Aaron K. Aragaki[2], Dennis Shaw[4], Thomas Bird[5], Janice Holton[6], Christopher Turner[7], Stephen J. Tapscott[3], Sarah J. Tabrizi[8], Anthony H. Schapira[5,6], Charles Kooperberg[2] and James M. Olson[1]

[1]Clinical Research Division, [2]Public Health Sciences Division, [3]Human Biology Division, Fred Hutchinson Cancer Research Center, Seattle, WA 98109, USA, [4]Department of Radiology, [5]Department of Neurology, University of Washington, Seattle, WA 98195, USA, [6]Department of Neuroscience, Institute of Neurology, University College London, Queen Square, London WC1N 3BG, UK, [7]University Department of Clinical Neurosciences, Royal Free and University College Medical School, UCL, London NW3 2PF, UK and [8]Department of Neurodegenerative Disease/MRC Prion Unit Institute of Neurology, National Hospital for Neurology and Neurosurgery, Queen Square, London WC1N 3BG, UK

Received March 29, 2005; Revised April 29, 2005; Accepted May 6, 2005

Huntington's disease (HD) is an incurable and fatal neurodegenerative disorder. Improvements in the objective measurement of HD will lead to more efficient clinical trials and earlier therapeutic intervention. We hypothesized that abnormalities seen in the R6/2 mouse, a greatly accelerated HD model, might highlight subtle phenotypes in other mouse models and human HD. In this paper, we identify common gene expression changes in skeletal muscle from R6/2 mice, *Hdh*$^{CAG(150)}$ homozygous knock-in mice and HD patients. This HD-triggered gene expression phenotype is consistent with the beginnings of a transition from fast-twitch to slow-twitch muscle fiber types. Metabolic adaptations similar to those induced by diabetes or fasting are also present but neither metabolic disorder can explain the full phenotype of HD muscle. The HD-induced gene expression changes reflect disease progression. This raises the possibility that muscle gene expression may be used as an objective biomarker to complement clinical HD-rating systems. Furthermore, an understanding of the molecular basis of muscle dysfunction in HD should provide insight into mechanisms involved in neuronal abnormalities and neurodegeneration.

INTRODUCTION

Huntington's disease (HD) is an autosomal dominant neurodegenerative disorder that has an incidence of roughly one per 10 000 in populations of western European descent (1). Typically, symptoms present during the third and fourth decades and progress inexorably, with death occurring 10–20 years after clinical onset. HD is one of the polyglutamine-related neurodegenerative diseases: disorders that include dentatorubral-pallidoluysian atrophy (DRPLA), X-linked spinal-bulbar muscular atrophy and at least six spinocerebellar ataxias (2). All of these disorders have a similar genetic basis, an expansion of a glutamine-encoding CAG-repeat, yet each is characterized by a different neuropathology. The hallmark neuropathology of HD is the severe and preferential loss of striatal medium spiny neurons, although localized cortical atrophy also occurs (1).

The first mouse models of HD were transgenic animals expressing exon-1 of the human *huntingtin* gene (3). The best studied of these, the R6/2 line, begins to exhibit behavioral and motor deficits about 6 weeks after birth. Subsequently, the phenotype of R6/2 mice develops rapidly, manifesting tremor, clasping, convulsions, weight loss, diabetes and behavioral abnormalities. Their life span is typically only 12–15 weeks (3,4). Other mouse models designed to faithfully reproduce the genetic defect in human HD have been made by inserting CAG repeats into the mouse *huntingtin* gene. These 'knock-in' HD animals have normal life spans and show subtle phenotypes relative to R6/2 mice (4,5). These mice may model the earlier stages of human HD, whereas the

*To whom correspondence should be addressed. Tel: +1 2066675681; Fax: +1 2066672917; Email: astrand@fhcrc.org

R6/2 mouse may recapitulate later stages or the rare juvenile form of human HD, which generally has a more severe clinical picture than adult-onset HD (1). The various mouse models of HD are now being used to screen potential treatments. However, due to their less dramatic phenotypes, preclinical trials involving knock-in HD mice require more time, material and money than trials involving R6/2 mice. Similarly, human clinical studies are complicated by the fact that the disease progresses fairly slowly and the current clinical rating scales are not sensitive enough to detect changes over short periods of time (6,7). The limitations of current methods of assessing HD patients necessitate large clinical trials of long duration. Thus, the development of objective biomarker measurements of HD is of importance, as these may improve the power and cost-effectiveness of drug trials.

Microarray profiling of gene expression can capture a broad view of direct and indirect effects related to polyglutamine toxicity in tissues from mice and humans. We hypothesized that abnormalities in the R6/2 mouse could guide a search for subtle phenotypes in other mouse models and human HD. The skeletal muscle is an accessible tissue that responds to hormonal, metabolic and neural inputs. Atrophy of skeletal muscle had been noted in the R6/2 mouse (8,9) and wasting is commonly seen late in human HD (1). The muscle, therefore, seemed a reasonable tissue to examine for gene expression changes that might be developed into HD biomarkers.

We have previously published a short list of gene expression changes in muscle from a small study on 8-week-old R6/2 mice (10). Here, we expand on that work by profiling skeletal muscle from older R6/2 mice. We use these profiles to define a molecular phenotype of gene expression changes associated with HD in skeletal muscle. In the mice, the gene expression changes are amplified as the disease progresses. We demonstrate that the phenotype is not merely a consequence of diabetes or weight loss and go on to show that the same phenotype can be observed in $Hdh^{CAG(150)}$ knock-in mice and muscle biopsies from human HD patients. The gene expression changes we describe seem to be universal characteristics of HD muscle and, as such, likely reflect fundamental mechanisms of disease. This makes muscle gene expression or some other biochemical assay of muscle function a good candidate for an HD biomarker.

RESULTS

Defining the molecular phenotype of HD muscle

The primary interest in beginning these studies was to determine whether gene expression changes could be detected in human HD muscle. Muscle biopsies are not commonly collected from HD patients. Thus, faced with the prospect of a small microarray study in the context of human variability, we attempted to gather power from the R6/2 HD model under the hypothesis that changes in the mice may illuminate the human phenotype.

The R6/2 mice begin to be distinguishable from their wild-type siblings around the age of 6 weeks. They gradually develop diabetes, progressively weigh less than normal and toward the end of their lives suffer a more precipitous loss of weight (3,11–14). Weight loss and diabetes are known to influence muscle gene expression (15–17). To demonstrate that the R6/2 skeletal muscle gene expression phenotype was not a trivial byproduct of diabetes, 8-week-old R6/2 mice were implanted with sustained-release insulin pellets or placebo pellets, whereas wild-type controls were implanted with placebo. These mice were sacrificed at 11 weeks of age. To control for weight loss effects, an additional cohort of control mice was fasted 2 days prior to sacrifice. These fasted mice lost 20% of their body weight and on average weighed the same as the R6/2 mice (data not shown). Skeletal muscle gene expression profiles from the fed R6/2 + placebo, fed R6/2 + insulin and fasted control mice were then compared with a common reference of fed control + placebo mice (complete analysis results can be found in the Supplementary Material; complete analysis and raw array data can be found at: http://HDBase.org).

Figure 1 shows intersections of probe sets meeting the $P < 0.001$ criteria for differential expression in each group relative to fed controls. There was extremely high concordance between the placebo- and insulin-treated R6/2 mice. Only one of the 1507 probe sets in the intersection of those two comparisons was changed in opposite directions. Because controlling blood glucose levels had very little effect on the R6/2 muscle phenotype, forces other than diabetes seemed to be driving the gene expression changes.

A severe fast induced many changes in muscle gene expression in wild-type mice. Figure 1 shows that although many of these were shared with the R6/2 phenotype, fasting captured only about one-third (573/1905) of the R6/2 phenotype. In addition, ~10% of the 573 genes in the R6/2–fasting intersection were discordantly affected. Finally, direct comparison of R6/2 with fasted-control mice demonstrated roughly as many differentially expressed probe sets (2033) as the R6/2 to fed–control comparison (1905). Only 74 probe sets met the $P < 0.001$ criteria in direct comparison of R6/2 + insulin and R6/2 skeletal muscle (Supplementary Material). We concluded that although both diabetes and weight loss may contribute to the muscle phenotype, neither can explain the complete set of skeletal muscle gene expression changes seen in R6/2 mice.

To confirm the changes seen in R6/2 mice at 11 weeks and refine the HD muscle phenotype, profiles from 15-week-old R6/2 and matched controls were collected (Supplementary Material). Of the 1905 differentially expressed probe sets in the 11-week profile, 1468 met the $P < 0.05$ criteria in the independent 15-week profile. This is substantially more than the approximately 95 probe sets (0.05×1905) that would be expected by chance. In addition, only two of the 1468 probe sets were incongruently expressed in the two profiles. The 15-week profile thus confirmed hundreds of gene expression changes identified in the profile of 11-week-old R6/2 skeletal muscles.

To define the HD muscle phenotype, probe sets were ranked by the absolute value of the sum of the moderated *t*-statistics (18) in the 11-week R6/2-to-control and 15-week R6/2-to-control comparisons. The 75 highest ranked named increasing genes and 75 highest ranked decreasing genes are shown in Table 1. Over-represented functional groups were identified in the top 100, 200 and 500 ranked probe sets using the online EASE tool (http://apps1.niaid.nih.gov/david/) (19). As may be

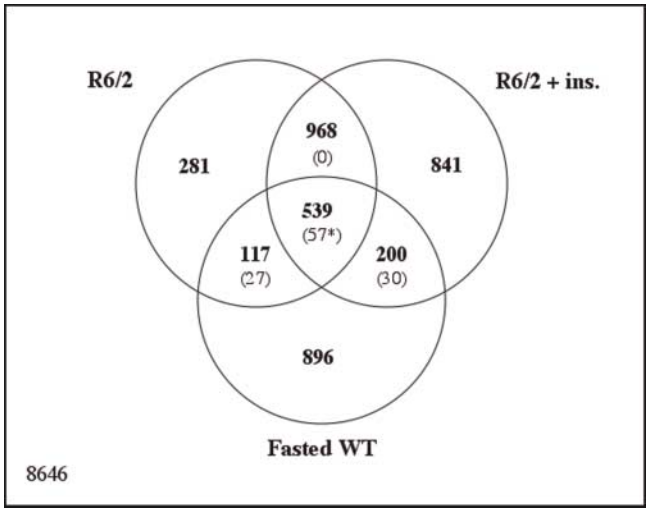

Figure 1. Venn diagram of probe sets meeting $P < 0.001$. Affymetrix U74Av2 arrays containing 12 488 probe sets were used to make gene expression profiles of quadriceps muscle from three treatment groups and a control group of wild-type mice. Each group contained four male mice. Sustained release insulin or placebo pellets were implanted subcutaneously into 8-week-old R6/2 and wild-type mice. These were subsequently sacrificed at an age of 11 weeks. The profiles from fed placebo treated R6/2, fed insulin treated R6/2, and fasted wild-type mice were compared with fed placebo treated wild-type mice. The numbers of probe sets meeting a $P < 0.001$ criteria in the three pair-wise comparisons of treatment to control are shown. Numbers in parentheses indicate the number of probes changed in opposite directions within the intersection. Asterisk indicates 56 of 57 discordant changes due to the fasting phenotype.

inferred from inspection of the gene lists in Table 1, significant over-representation was seen in the decreased list for genes encoding 'fast' muscle fiber proteins and glycolytic enzymes. Decreases in 'fast' myofibrillar protein genes were noted previously in profiles from 8-week-old R6/2 skeletal muscle generated as part of a small spotted array expression profile (10). Increased genes fell into groups for 'slow' muscle proteins, lipid catabolism, protein synthesis and folding, heat-shock, proteasome and other types of stress-response. Taken together, these patterns of increases and decreases in functional groups are consistent with a transition from fast type II glycolytic muscle fibers to slow type I oxidative muscle fibers (20,21). On the basis of histochemical evidence, such a transition in R6/2 skeletal muscle was recently proposed (9).

To demonstrate that the skeletal muscle phenotype is progressive and further confirm the array data, northern blots were performed using total RNA isolated from R6/2 and control mice (Fig. 2). Three genes were examined: *lactate dehydrogenase A* (*LDHA*), the predominant LDH isoform in skeletal muscle (22); *alpha-actinin-2* (*ACTN2*), which is expressed in all mouse muscle fibers and *alpha-actinin-3* (*ACTN3*), an actinin isoform expressed in a subset of type II fast fibers (23). Like *ACTN3*, *LDHA* is more highly expressed in mouse fast-twitch fibers (24). *LDHA* and *ACTN3* are significant decreases in the R6/2 array data and appear in Table 1. *ACTN2* does not appear as a statistically significant increase in the R6/2 array data analyzed with Robust Multi-array Average (RMA) software (18,25–27), but does appear as a significant increase when using Affymetrix MAS 5.0 software (data not shown). Consistent with repression of fast-twitch fiber genes, *LDHA* and *ACTN3* clearly decreased relative to normal in R6/2 mice. *ACTN2* increased in R6/2 mice, a result that suggests *ACTN2* is preferentially expressed in mouse slow-twitch fibers or fibers adapting to HD-mediated effects. The differences between R6/2 and control mice became greater with age, demonstrating progression of the muscle gene expression phenotype in concert with the other neurological and behavioral phenotypes in R6/2 mice.

Human and mouse HD muscle exhibit a common program of gene expression changes

To explore gene expression changes in human HD, we obtained muscle biopsies from eight HD patients and seven controls. The patients' motor and cognitive symptoms as measured by the Unified Huntington's Disease Rating Scale (6,7), ranged from essentially normal to severely affected (Table 2). None of the biopsy donors had frank diabetes or was emaciated, so it was unlikely that human HD muscle gene expression changes would be caused by diabetes or weight loss. After analysis, only 50 probe sets exceeded the $P < 0.001$ criteria. As approximately 22 would be expected by chance, one might assume that these 50 probe sets would have a high false discovery rate. The 75 highest ranked non-redundant named increases and 75 highest ranked decreases are shown in Table 3 (complete data in Supplementary Material and at http://HDBase.org). Inspection of Tables 1 and 3 reveals several common themes between mouse and human HD muscle. Both the mouse and human HD gene lists noted reduced glycolytic enzyme and 'fast' myofibrillar mRNAs, whereas increased expression was found for lipid metabolism and 'slow' myofibrillar messages. As these pathways were affected in R6/2 mice in exactly the same fashion, the trends in the small human microarray study seemed unlikely to be due solely to chance.

The simple functional analysis described earlier looks only at intersections between statistically significant changes in R6/2 and human muscle. If R6/2 and human HD muscle shared a similar biology, trends in orthologous genes should be similar even if few genes were flagged as statistically significant in this small human study. We used two statististical methods using different bioinformatic data-cleaning steps to detect common trends across species and array platforms. In the first approach, the probe sets on the mouse and human arrays were collapsed into a set of unique genes with one-to-one matching of genes between species. On the basis of their moderated *t*-statistics (18), the mouse and human genes were separately ranked to generate two independent rank-ordered lists. A one-sided Mann–Whitney test (28) was then applied to see whether the human genes corresponding to the most significantly HD-affected mouse genes were included in the extremes of the rank-ordered human genes. Up-regulated and down-regulated genes were analyzed separately. Considering the most significant 250 mouse increases and decreases, we, respectively, obtained permutation-based *P*-values of 0.25 and 0.0004 for relatedness between mouse and human HD. This represented very strong evidence for a

Table 1. Top gene expression changes in muscle from R6/2 mice

Decreased[a]			Increased[b]		
Probe set ID	Gene	Symbol	Probe set ID	Gene	Symbol
103297_at	*6-phosphofructo-2-kinase/fructose-2,6-biphosphatase 1*	*Pfkfb1*	160171_f_at	*acyl-coenzyme A thioesterase 2, mitochondrial*	*Acate2*
160641_at	*6-phosphofructo-2-kinase/fructose-2,6-biphosphatase 3*	*Pfkfb3*	94850_at	***acyl-coenzyme A thioesterase 3, mitochondrial***	***Acate3***
162388_r_at	a disintegrin and metalloprotease domain 5	*Adam5*	104011_at	*aldehyde oxidase 1*	*Aox1*
162164_f_at	*actinin alpha 3*	*Actn3*	104671_at	*AMP deaminase 3*	*Ampd3*
93560_at	*acylphosphatase 1, erythrocyte (common) type*	*Acyp1*	98476_at	*ankyrin 3, epithelial*	*Ank3*
96801_at	*adenylate kinase 1*	*Ak1*	93252_at	***B-cell receptor-associated protein 31***	***Bcap31***
98435_at	*adenylosuccinate synthetase 1, muscle*	*Adss1*	101514_at	*Bet3 homolog (S. cerevisiae)*	*Bet3*
161889_f_at	***aldolase 1, A isoform***	***Aldo1***	100458_at	*brain protein 14*	*Brp14*
100440_f_at	*ankyrin 1, erythroid*	*Ank1*	94878_at	*BTB (POZ) domain containing 1*	*Btbd1*
104701_at	*basic helix–loop–helix domain containing, class B2*	*Bhlhb2*	102248_f_at	*calcium/calmodulin-dependent serine protein kinase*	*Cask*
101078_at	*basigin*	*Bsg*	102048_at	*cardiac responsive adriamycin protein*	*Crap*
100539_at	*brain acyl-CoA hydrolase*	*Bach*	102952_g_at	*CASP2 and RIPK1 domain containing adaptor with death domain*	*Cradd*
101128_at	*calcium channel, voltage-dependent, L type, alpha 1S subunit*	*Cacna1s*	160479_at	*catalase*	*Cat*
102426_at	*calsequestrin 1*	*Casq1*	101963_at	*cathepsin L*	*Ctsl*
100600_at	*CD24a antigen*	*Cd24a*	160493_at	*Cd63 antigen*	*Cd63*
101403_at	*chemokine (C-C motif) ligand 25*	*Ccl25*	100021_at	***cholinergic receptor, nicotinic, alpha polypeptide 1***	***Chrna1***
162276_i_at	*complement component 1, q subcomponent, beta polypeptide*	*C1qb*	93705_at	*cholinergic receptor, nicotinic, beta polypeptide 1 (muscle)*	*Chrnb1*
161569_f_at	***creatine kinase, muscle***	***Ckm***	99191_at	*CREBBP/EP300 inhibitory protein 1*	*Cri1*
160841_at	*D site albumin promoter binding protein*	*Dbp*	98478_at	*cyclin G2*	*Ccng2*
93188_at	*dickkopf homolog 3 (Xenopus laevis)*	*Dkk3*	94881_at	*cyclin-dependent kinase inhibitor 1A (P21)*	*Cdkn1a*
101090_at	*fibrillin 1*	*Fbn1*	95682_at	*damage specific DNA binding protein 1*	*Ddb1*
103995_at	*fibroblast growth factor binding protein 1*	*Fgfbp1*	160074_at	*dopa decarboxylase*	*Ddc*
102967_at	*ganglioside-induced differentiation-associated-protein 1*	*Gdap1*	97740_at	*dual specificity phosphatase 16*	*Dusp16*
97430_at	*glucose-6-phosphatase, transport protein 1*	*G6pt1*	103891_i_at	*ELL-related RNA polymerase II, elongation factor*	*Ell2*
101214_f_at	*glyceraldehyde-3-phosphate dehydrogenase*	*Gapd*	93754_at	*enoyl coenzyme A hydratase 1, peroxisomal*	*Ech1*
161753_f_at	*glycerol-3-phosphate dehydrogenase 1 (soluble)*	*Gpd1*	102774_at	*epidermal growth factor*	*Egf*
95593_at	*golgi phosphoprotein 2*	*Golph2*	99101_at	*eukaryotic translation initiation factor 3, subunit 7 (zeta)*	*Eif3s7*
162346_f_at	*histocompatibility 2, class II, locus DMa*	*H2-DMa*	94297_at	*FK506 binding protein 5*	*Fkbp5*
93583_s_at	*immunoglobulin heavy chain 6 (heavy chain of IgM)*	*Igh-6*	103254_at	*FLN29 gene product*	*Fln29*
93895_s_at	*inositol 1,4,5-triphosphate receptor 1*	*Itpr1*	94206_at	*gene rich cluster, C10 gene*	*Grcc10*
95546_g_at	*insulin-like growth factor 1*	*Igf1*	93009_at	*glutathione S-transferase, mu 2*	*Gstm2*
100566_at	*insulin-like growth factor binding protein 5*	*Igfbp5*	102292_at	***growth arrest and DNA-damage-inducible 45 alpha***	***Gadd45a***
94534_at	*isocitrate dehydrogenase 3 (NAD+) alpha*	*Idh3a*	160714_at	*growth factor receptor bound protein 2-associated protein 1*	*Gab1*
160341_at	*JTV1 gene*	*Jtv1*	95359_at	*heat shock protein 1, beta*	*Hspcb*
99536_at	*kinase interacting protein 2*	*Kip2*	94428_at	*ilvB (bacterial acetolactate synthase)-like*	*Ilvbl*
96072_at	*lactate dehydrogenase 1, A chain*	*Ldh1*	104264_at	*LPS-responsive beige-like anchor*	*Lrba*
101409_at	*ligatin*	*Lgtn*	160138_at	*Max interacting protein 1*	*Mxi1*
160354_at	*LIM domain binding 3*	*Ldb3*	96703_at	*melanoma antigen, family D, 1*	*Maged1*
93642_at	*longevity assurance homolog 1 (*Saccharomyces cerevisiae*)*	*Lass1*	94289_r_at	*melanoma antigen, family D, 2*	*Maged2*
102828_at	*mitogen activated protein kinase kinase 6*	*Map2k6*	160287_at	*microtubule-associated protein 1 light chain 3*	*Map1lc3*
103838_at	*mitsugumin 29*	*Mg29*	92795_at	*microtubule-associated protein 4*	*Mtap4*
102061_at	*myeloid leukemia factor 1*	*Mlf1*	102431_at	*microtubule-associated protein tau*	*Mapt*
100614_at	*myoglobin*	*Mb*	101013_at	*ornithine decarboxylase antizyme*	*Oaz1*
162101_f_at	***myosin light chain, phosphorylatable, fast muscle***	***Mylpf***	104070_at	*p300/CBP-associated factor*	*Pcaf*
98488_at	*myosin, heavy polypeptide 4, skeletal muscle*	*Myh4*	95731_at	***p53 regulated PA26 nuclear protein***	***Pa26***
104555_at	*myozenin 1*	*Myoz1*	96765_at	*paternally expressed 3*	*Peg3*
160284_at	*NADH dehydrogenase (ubiquinone) 1 alpha subcomplex 10*	*Ndufa10*	94485_at	*peroxisomal delta3, delta2-enoyl-coenzyme A isomerase*	*Peci*
98507_at	*nuclear receptor subfamily 1, group D, member 1*	*Nr1d1*	92452_at	*phosphatidylinositol 3-kinase, catalytic, alpha polypeptide*	*Pik3ca*
96720_f_at	*parvalbumin*	*Pva*	95486_at	*phosphatidylserine receptor*	*Ptdsr*
161348_r_at	*PDZ and LIM domain 1 (elfin)*	*Pdlim1*	160793_at	*POU domain, class 6, transcription factor 1*	*Pou6f1*
92731_at	*pentaxin-related gene*	*Ptx3*	98150_at	*RAB11B, member RAS oncogene family*	*Rab11b*

92599_at	*phosphoglycerate mutase 2*	*Pgam2*	104108_at	***Rab6 interacting protein 1***	***Rab6ip1***
102725_at	*K voltage-gated channel, shaker-related subfamily, beta 1*	*Kcnab1*	93255_at	*ralA binding protein 1*	*Ralbp1*
94305_at	*procollagen, type I, alpha 1*	*Col1a1*	96747_at	*ras homolog gene family, member U*	*Arhu*
162459_f_at	*procollagen, type VI, alpha 1*	*Col6a1*	93020_at	*reduced expression 3*	*Rex3*
93517_at	*procollagen, type VI, alpha 2*	*Col6a2*	97948_at	*retinoblastoma 1*	*Rb1*
99637_at	*procollagen, type XV*	*Col15a1*	160977_at	*Rho guanine nucleotide exchange factor (GEF) 5*	*Arhgef5*
103975_at	*protein related to DAN and cerberus*	*Prdc*	100959_at	*S100 calcium binding protein A13*	*S100a13*
160480_at	*protein tyrosine phosphatase, receptor type, S*	*Ptprs*	98553_at	*sarcolemma associated protein*	*Slmap*
92237_at	*retinoid X receptor gamma*	*Rxrg*	98905_at	*septin 7*	*Sept7*
100003_at	*ryanodine receptor 1, skeletal muscle*	*Ryr1*	160068_at	*sin3 associated polypeptide*	*Sap30*
101489_at	***S-adenosylmethionine decarboxylase 1***	***Amd1***	95456_r_at	*split hand/foot deleted gene 1*	*Shfdg1*
161530_r_at	*semaphorin 4A*	*Sema4a*	102012_at	*src family associated phosphoprotein 2*	*Scap2*
92639_at	*serine/threonine kinase 6*	*Stk6*	92807_at	*thioredoxin 1*	*Txn1*
96205_at	*SH3-binding domain glutamic acid-rich protein*	*Sh3bgr*	99985_at	*thioredoxin reductase 1*	*Txnrd1*
99320_at	*sialyltransferase 8 (alpha-2, 8-sialyltransferase) E*	*Siat8e*	93789_s_at	*transcriptional regulator, SIN3B (yeast)*	*Sin3b*
102314_at	*solute carrier family 2 (facilitated glucose transporter), 4*	*Slc2a4*	94266_at	*tumor necrosis factor receptor superfamily, member 12a*	*Tnfrsf12a*
99057_at	*thymus cell antigen 1, theta*	*Thy1*	101255_at	*ubiquitin B*	*Ubb*
99566_at	*triosephosphate isomerase*	*Tpi*	92818_at	*ubiquitin-activating enzyme E1C*	*Ube1c*
100605_at	*tropomyosin 2, beta*	*Tpm2*	94267_i_at	*ubiquitin-like 5*	*Ubl5*
93532_at	***troponin I, skeletal, fast 2***	***Tnni2***	100964_at	*vesicle transport through interaction with t-SNAREs 1B*	*Vti1b*
92885_at	***troponin T3, skeletal, fast***	***Tnnt3***	98767_at	*YY1 transcription factor*	*Yy1*
104682_at	*tubulin, alpha 8*	*Tuba8*	99052_at	*zinc finger homeobox 1a*	*Zfhx1a*
96534_at	*very low density lipoprotein receptor*	*Vldlr*	94780_at	*zinc finger protein 288*	*Zfp288*
103783_at	*xenotropic and polytropic retrovirus receptor 1*	*Xpr1*	92974_at	*zinc finger protein 37*	*Zfp37*

The vast majority of these genes met the $P < 0.001$ criteria in the completely independent 11- and 15-week R6/2 gene expression profiles. A few genes had consistent changes with a P-value slightly larger than 0.001 in one experiment matched by a P-value much smaller than 0.001 in the other experiment. These gene lists represent the top few of the many hundred gene expression changes detected in R6/2 skeletal muscle. See Supplementary data or http://HDBase.org for complete gene expression data. Genes in bold type represent previously published gene expression changes seen in 8-week-old R6/2 mice (10).

[a]The top 75 non-redundant named decreasing genes in R6/2 quadriceps muscle.

[b]The top 75 non-redundant named increasing genes.

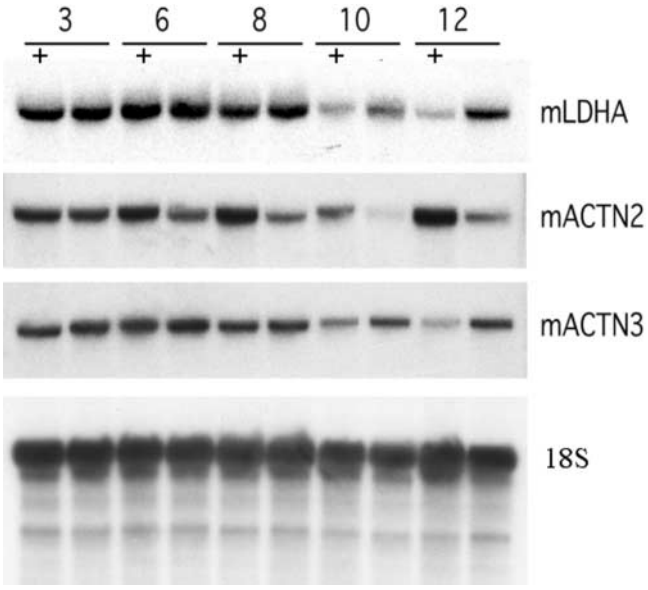

Figure 2. Time course and confirmation of R6/2 skeletal muscle gene expression changes. Quadriceps muscle RNA from male R6/2 and wild-type littermates of several ages was isolated and used for northern analysis. The age in weeks is indicated above each pair of lanes. '+' indicates R6/2 RNA. Duplicate blots containing 10 μg of total RNA per lane were probed for *alpha-actinin 2 (mACTN2)* and *alpha-actinin 3 (mACTN3)*. The *mACTN2* blot was subsequently stripped and reprobed for *lactate dehydrogenase A (mLDHA)*. The *mACTN3* blot was stripped and reprobed for 18S ribosomal RNA as a loading control.

common program of skeletal muscle gene repression in mouse and human HD.

In a second approach to demonstrating commonality, the mouse probe sets were ranked by the absolute value of the sum of moderated *t*-statistics (18) in the 11- and 15-week profiles. This rank-ordering was then applied to all orthologous human probes. When a mouse probe mapped to multiple human probes, the signals of the redundant human probes were averaged. Finally, if the gene decreased in mouse HD, the human signals were multiplied by -1. This created a list for each human HD case and control with one-to-one correspondence between mouse and human genes all rank-ordered by the R6/2 significance. We then implemented a 'running *t*-test'. For $g = 1$ to n, signals for the first g genes were averaged (as we normalized gene expression using RMA, all expressions were on the same scale) and a series of *P*-values calculated using a regular *t*-test on the averages. If there were trends in the data that distinguished the HD group from controls, *P*-values for the averages would likely become smaller than *P*-values for individual genes as the HD signal 'added up'. Furthermore, the running *P*-value should reach a minimum near the top of the list and the significance of the signal should be persistent. If the mouse and human lists were not biologically related, the running *P*-values would be expected to quickly exhibit a pattern similar to a random walk about some insignificant *P*-value. Figure 3 shows that the mouse and human data were biologically congruent. *P*-values reached a minimum of $P = 0.00056$ and based upon 10 000 permutations of the genes, the frequency of observing a $P \leq 0.00056$ among the first 100 genes of a ranked list was $P = 0.034$. Thus, two statistical approaches with different bioinformatic data clean-up steps provided us with strong evidence for a common program of skeletal muscle gene expression in mouse and human HD. The similarities between R6/2 and human HD were deepest in the genes that decreased, genes associated with fast-twitch muscle fibers and glycolysis.

Table 2. Clinical data from muscle biopsy donors

Donor	Age	Gender	Clinical stage	Motor score	Cognitive score
HD 001	56	F	3	49	167
HD 002	57	M	3	70	68
HD 003	36	M	0	2	260
HD 004	37	M	1	35	234
HD 008	61	F	nd	nd	nd
HD 009	59	M	nd	nd	nd
HD 010	40	F	3[a]	nd	nd
HD 012	44	F	3[a]	nd	nd
C 001	59	F			
C 002	65	M			
C 003	36	M			
C 004	39	M			
C 005	44	M			
C 006	27	M			
C 007	33	M			

The age and gender of all muscle biopsy donors plus, when available, Unified Huntington's Disease Rating Scale scores of the HD patients are shown. Clinical stage scores range from 0, least affected, to 5, severely affected. Motor scores begin at 0 and tend to increase with advancing HD. Average cognitive scores are typically near 230 and diminish with advancing HD.

Muscle gene expression changes are not due to adipocyte contamination

Infiltration or contamination of the muscle biopsies with adipose cells was a plausible trivial explanation for the changes seen in HD muscle. To examine this possibility, we profiled subcutaneous adipose tissue from three HD patients. If HD muscle contained higher numbers of adipose cells, one would expect adipose markers, i.e. genes greatly more expressed in adipose tissue than muscle, to contribute substantially to the set of genes apparently increasing in HD muscle. Probe sets for adipose markers were identified by rank-ordering the differences of the mean human adipose and muscle signals. Of the top 1000 'adipose' probe sets, respectively, only 6, 14 and 20 were found within the top 100, 250 and 500 human HD muscle increases (Supplementary Material). Similar numbers were found in the top HD decreases. Because the vast majority of top changes, both increases and decreases, in the human expression profile were muscle genes, we concluded that the HD signature identified in human skeletal muscle biopsies was not reflecting skewed ratios of adipose and skeletal muscle cells.

Confirmation of human array data

To confirm changes in human HD, we performed a northern blot for *LDHA* on total muscle RNA from four age- and

Table 3. Top gene expression changes in human HD muscle

Decreased[a]			Increased[b]		
Probe set ID	Gene	Symbol	Probe set ID	Gene	Symbol
207537_at	***6-phosphofructo-2-kinase/fructose-2,6-biphosphatase 1***	***PFKFB1***	204607_at	*3-hydroxy-3-methylglutaryl-coenzyme A synthase 2*	*HMGCS2*
202587_s_at	***adenylate kinase 1***	***AK1***	205412_at	*acetyl-coenzyme A acetyltransferase 1*	*ACAT1*
205444_at	*ATPase, Ca^{2+} transporting, cardiac muscle, fast twitch 1*	*ATP2A1*	203862_s_at	***actinin, alpha 2***	***ACTN2***
203795_s_at	*B-cell CLL/lymphoma 7A*	*BCL7A*	201425_at	*aldehyde dehydrogenase 2 family (mitochondrial)*	*ALDH2*
212963_at	*beta-amyloid binding protein precursor*	*BBP*	221589_s_at	*aldehyde dehydrogenase 6 family, member A1*	*ALDH6A1*
209770_at	*butyrophilin, subfamily 3, member A1*	*BTN3A1*	221232_s_at	*ankyrin repeat domain 2 (stretch responsive muscle)*	*ANKRD2*
221249_s_at	*C/EBP-induced protein*	*LOC81558*	200844_s_at	*antioxidant protein 2*	*AOP2*
208377_s_at	*calcium channel, voltage-dependent, alpha 1F subunit*	*CACNA1F*	200940_s_at	*arginine-glutamic acid dipeptide (RE) repeats*	*RERE*
205692_s_at	*CD38 antigen (p45)*	*CD38*	216008_s_at	*ariadne homolog 2 (Drosophila)*	*ARIH2*
212624_s_at	*chimerin (chimaerin) 1*	*CHN1*	201089_at	*ATPase, H^+ transporting, lysosomal, V1 subunit B, isoform 2*	*ATP6V1B2*
204775_at	*chromatin assembly factor 1, subunit B (p60)*	*CHAF1B*	203140_at	*B-cell CLL/lymphoma 6 (zinc finger protein 51)*	*BCL6*
204363_at	*coagulation factor III (thromboplastin, tissue factor)*	*F3*	219966_x_at	*BTG3 associated nuclear protein*	*BANP*
216893_s_at	*collagen, type IV, alpha 3 (Goodpasture antigen)*	*COL4A3*	207317_s_at	*calsequestrin 2 (cardiac muscle)*	*CASQ2*
212793_at	*dishevelled associated activator of morphogenesis 2*	*DAAM2*	210070_s_at	*carnitine palmitoyltransferase 1B (muscle)*	*CPT1B*
202866_at	*DnaJ (Hsp40) homolog, subfamily B, member 12*	*DNAJB12*	209508_x_at	*CASP8 and FADD-like apoptosis regulator*	*CFLAR*
208430_s_at	*dystrobrevin, alpha*	*DTNA*	218170_at	*CGI-111 protein*	*CGI-111*
214266_s_at	*enigma (LIM domain protein)*	*ENIGMA*	217868_s_at	*CGI-81 protein*	*DREV1*
204483_at	*enolase 3, (beta, muscle)*	*ENO3*	205022_s_at	*checkpoint suppressor 1*	*CHES1*
211165_x_at	*EphB2*	*EPHB2*	209283_at	*crystallin, alpha B*	*CRYAB*
211603_s_at	*ets variant gene 4 (E1A enhancer binding protein, E1AF)*	*ETV4*	213348_at	*cyclin-dependent kinase inhibitor 1C (p57, Kip2)*	*CDKN1C*
221664_s_at	*F11 receptor*	*F11R*	202552_s_at	*cysteine-rich motor neuron 1*	*CRIM1*
210950_s_at	*farnesyl-diphosphate farnesyltransferase 1*	*FDFT1*	201431_s_at	*dihydropyrimidinase-like 3*	*DPYSL3*
204579_at	*fibroblast growth factor receptor 4*	*FGFR4*	202942_at	*electron-transfer-flavoprotein, beta polypeptide*	*ETFB*
219327_s_at	*G protein-coupled receptor, family C, group 5, member C*	*GPRC5C*	209368_at	*epoxide hydrolase 2, cytoplasmic*	*EPHX2*
208308_s_at	*glucose phosphate isomerase*	*GPI*	207981_s_at	*estrogen-related receptor gamma*	*ESRRG*
217289_s_at	*glucose-6-phosphatase*	*G6PC*	218751_s_at	*F-box and WD-40 domain protein 7*	*FBXW7*
M33197_M_at	***glyceraldehyde-3-phosphate dehydrogenase***	***GAPD***	206603_at	*facilitated glucose transporter*	*SLC2A4*
213706_at	***glycerol-3-phosphate dehydrogenase 1 (soluble)***	***GPD1***	204359_at	*fibronectin leucine rich transmembrane protein 2*	*FLRT2*
202947_s_at	*glycophorin C (Gerbich blood group)*	*GYPC*	211979_at	*G protein-coupled receptor 107*	*GPR107*
209342_s_at	*in. kappa light polypeptide gene enhancer in B-cells, kinase beta*	*IKBKB*	213880_at	*G protein-coupled receptor 49*	*GPR49*
210547_x_at	*islet cell autoantigen 1, 69 kDa*	*ICA1*	209248_at	*growth hormone inducible transmembrane protein*	*GHITM*
206241_at	*karyopherin alpha 5 (importin alpha 6)*	*KPNA5*	200800_s_at	*heat shock 70 kDa protein 1A*	*HSPA1A*
200650_s_at	***lactate dehydrogenase A***	***LDHA***	211969_at	*heat shock 90 kDa protein 1, alpha*	*HSPCA*
211562_s_at	*leiomodin 1 (smooth muscle)*	*LMOD1*	209068_at	*heterogeneous nuclear ribonucleoprotein D-like*	*HNRPDL*
204357_s_at	*LIM domain kinase 1*	*LIMK1*	200593_s_at	*heterogeneous nuclear ribonucleoprotein U*	*HNRPU*
202068_s_at	*low density lipoprotein receptor*	*LDLR*	208808_s_at	*high-mobility group box 2*	*HMGB2*
209887_at	*MAD, mothers against decapentaplegic homolog 6 (Drosophila)*	*MADH6*	200943_at	*high-mobility group nucleosome binding domain 1*	*HMGN1*
213863_s_at	*mitochondrial ribosomal protein L9*	*MRPL9*	201007_at	*trifunctional protein, beta subunit*	*HADHB*
205448_s_at	*mitogen-activated protein kinase kinase kinase 12*	*MAP3K12*	201036_s_at	*L-3-hydroxyacyl-coenzyme A dehydrogenase, short chain*	*HADHSC*
202788_at	*mitogen-activated protein kinase-activated protein kinase 3*	*MAPKAPK3*	213564_x_at	*lactate dehydrogenase B*	*LDHB*
221779_at	*molecule interacting with Rab13*	*MIRAB13*	218574_s_at	*LIM and cysteine-rich domains 1*	*LMCD1*
204782_at	***myeloid leukemia factor 1***	***MLF1***	203549_s_at	*lipoprotein lipase*	*LPL*
207840_at	*natural killer cell receptor, immunoglobulin superfamily*	*BY55*	201155_s_at	*mitofusin 2*	*MFN2*
211143_x_at	*nuclear receptor subfamily 4, group A, member 1*	*NR4A1*	210017_at	*mucosa associated lymphoid tissue lymphoma translocation 1*	*MALT1*
213059_at	*old astrocyte specifically induced substance*	*OASIS*	205079_s_at	*multiple PDZ domain protein*	*MPDZ*
222304_x_at	*olfactory receptor, family 7, subfamily E, member 47 pseudogene*	*OR7E47P*	205826_at	*myomesin (M-protein) 2, 165 kDa*	*MYOM2*
205336_at	***parvalbumin***	***PVALB***	204737_s_at	*myosin, heavy polypeptide 7, cardiac muscle, beta*	*MYH7*
204448_s_at	*phosducin-like*	*PDCL*	215795_at	*myosin, heavy polypeptide 7B, cardiac muscle, beta*	*MYH7B*
210976_s_at	*phosphofructokinase, muscle*	*PFKM*	201319_at	*myosin, light polypeptide, regulatory, non-sarcomeric (20kD)*	*MLCB*

Continued

Table 3. Continued

Decreased[a]			Increased[b]		
Probe set ID	Gene	Symbol	Probe set ID	Gene	Symbol
205736_at	***phosphoglycerate mutase 2 (muscle)***	***PGAM2***	211476_at	*myozenin 2*	*MYOZ2*
221389_at	*phospholipase A2, group IIE*	*PLA2G2E*	219437_s_at	*nasopharyngeal carcinoma susceptibility protein*	*LZ16*
212955_s_at	*polymerase (RNA) II (DNA directed) polypeptide I, 14.5 kDa*	*POLR2I*	221691_x_at	*nucleophosmin (nucleolar phosphoprotein B23, numatrin)*	*NPM1*
45653_at	*polymerase delta-interacting protein 1*	*PDIP1*	202073_at	*optineurin*	*OPTN*
205902_at	*K inter./small conductance calcium-activated channel, N, 3*	*KCNN3*	204853_at	*origin recognition complex, subunit 2-like (yeast)*	*ORC2L*
213774_s_at	*protein phosphatase 1, regulatory (inhibitor) subunit 2*	*PPP1R2*	208690_s_at	*PDZ and LIM domain 1 (elfin)*	*PDLIM1*
206895_at	*protein phosphatase 1, regulatory (inhibitor) subunit 3A*	*PPP1R3A*	212392_s_at	*phosphodiesterase 4D interacting protein (myomegalin)*	*PDE4DIP*
201251_at	*pyruvate kinase, muscle*	*PKM2*	202880_s_at	*pleckstrin homology, Sec7 and coiled/coil domains 1*	*PSCD1*
204558_at	*RAD54-like (S. cerevisiae)*	*RAD54L*	207543_s_at	*procollagen-proline, 2-oxoglutarate 4-dioxygenase, alpha I*	*P4HA1*
204217_s_at	*reticulon 2*	*RTN2*	209296_at	*protein phosphatase 1B (formerly 2C), beta isoform*	*PPM1B*
205954_at	***retinoid X receptor, gamma***	***RXRG***	203997_at	*protein tyrosine phosphatase, non-receptor type 3*	*PTPN3*
203055_s_at	*Rho guanine nucleotide exchange factor (GEF) 1*	*ARHGEF1*	202151_s_at	*putative glialblastoma cell differentiation-related*	*GDBR1*
200850_s_at	*S-adenosylhomocysteine hydrolase-like 1*	*AHCYL1*	200864_s_at	*RAB11A, member RAS oncogene family*	*RAB11A*
212902_at	*SEC24 related gene family, member A (S. cerevisiae)*	*SEC24A*	218428_s_at	*REV1-like (yeast)*	*REV1L*
219197_s_at	*signal peptide, CUB domain, EGF-like 2*	*SCUBE2*	206306_at	*ryanodine receptor 3*	*RYR3*
207390_s_at	*smoothelin*	*SMTN*	200903_s_at	*S-adenosylhomocysteine hydrolase*	*AHCY*
207051_at	*solute carrier family 17 (sodium phosphate), member 4*	*SLC17A4*	222258_s_at	*SH3-domain binding protein 4*	*SH3BP4*
209363_s_at	*SRB7 suppressor of RNA polymerase B homolog (yeast)*	*SURB7*	208741_at	*sin3-associated polypeptide, 18 kDa*	*SAP18*
203019_x_at	*synovial sarcoma, X breakpoint 2 interacting protein*	*SSX2IP*	216103_at	*thioesterase, adipose associated*	*THEA*
200822_x_at	***triosephosphate isomerase 1***	***TPI1***	200792_at	*thyroid autoantigen 70 kDa (Ku antigen)*	*G22P1*
207643_s_at	*tumor necrosis factor receptor superfamily, member 1A*	*TNFRSF1A*	201515_s_at	*translin*	*TSN*
201689_s_at	*tumor protein D52*	*TPD52*	214365_at	*tropomyosin 3*	*TPM3*
218837_s_at	*ubiquitin-conjugating enzyme HBUCE1*	*LOC51619*	213201_s_at	*troponin T1, skeletal, slow*	*TNNT1*
209825_s_at	*uridine monophosphate kinase*	*UMPK*	201379_s_at	*tumor protein D52-like 2*	*TPD52L2*
205205_at	*v-rel reticuloendotheliosis viral oncogene homolog B*	*RELB*	205356_at	*ubiquitin specific protease 13 (isopeptidase T-3)*	*USP13*
220214_at	*zinc finger protein 215*	*ZNF215*	221485_at	*UDP-Gal:betaGlcNAc beta1,4-galactosyltransferase, pep. 5*	*B4GALT5*

See Supplementary data or http://HDBase.org for complete gene expression data. Genes in bold type appear in Table 1, the top R6/2 changes. *Alpha-actinin 2* does not appear in Table 1, but was shown to increase in R6/2 muscle by northern blot (Fig. 2).

[a]The top 75 non-redundant named decreasing genes in human HD vastus lateralis muscle.

[b]The top 75 non-redundant named increasing genes.

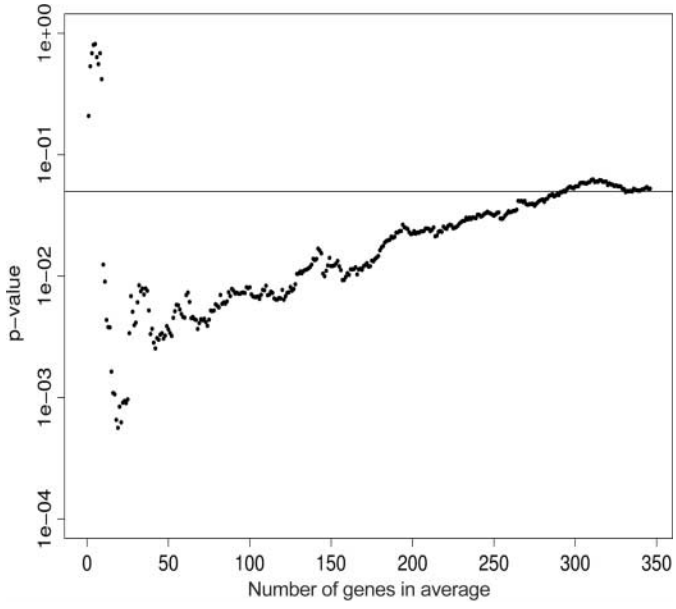

Figure 3. Running *t*-test *P*-values based on averaged human HD signal values rank-ordered according to the R6/2 data. Human probe sets orthologous to mouse probe sets were ranked by their significance in the R6/2 HD phenotype. If the probe set decreased in mouse HD, the human signals were multiplied by −1. A one-sided *t*-test was then sequentially performed on the average signal of the first *g* human genes. Each *t*-test was a comparison of the HD group and the control group. Nominal *P*-values for the HD-effect are plotted against *g*. The *P*-value plot does not behave as a random walk, indicating that the gene expression changes in mouse and human HD skeletal muscle are congruent and similar.

gender-matched cases and controls (Fig. 4). Even in the context of normal human variability, all of the HD cases clearly had lower levels of *LDHA* message than controls. This confirmed the decrease of *LDHA* indicated by the human HD array data. Reduced levels of *LDHA* mRNA in human HD parallels the R6/2 LDHA changes detected by independent microarray experiments and confirmed by northern analysis. We then re-examined *LDHA* and 12 other genes using semi-quantitative RT–PCR in the same set of matched cases and controls. The examined genes were selected to explore the inferred shifts from fast and slow fiber isoforms, sugar to lipid catabolism and induction of heat shock proteins. As shown in Table 4, we were able to confirm the direction of change predicted by microarray in 11 of the 13 genes examined by RT–PCR. Eight of the examined genes met statistical significance at $P < 0.05$ in the RT–PCR assays.

Impaired glucose homeostasis in $Hdh^{CAG(150)}$ knock-in mice

Observation of common changes in R6/2 mice and humans could, however unlikely, be dismissed as a microarray artifact so, we examined whether similar trends took place in a second HD mouse model. The $Hdh^{CAG(150)}$ knock-in model of HD shows subtle behavioral differences beginning at about 4 months of age (4,5). Their phenotype develops slowly and does not manifest as obviously as the R6/2 phenotype. We profiled skeletal muscle from 6-month-old homozygous

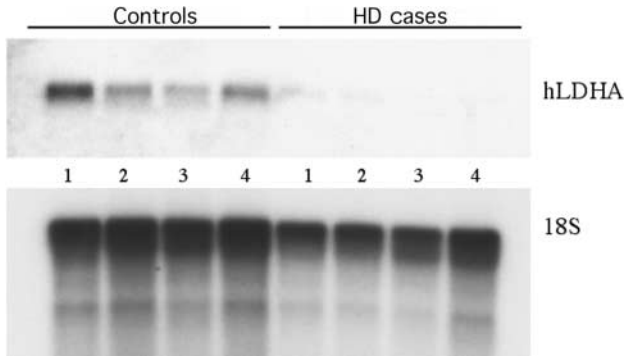

Figure 4. Northern blot of *lactate dehydrogenase A (hLDHA)* message levels in an age- and gender-matched subset of the human HD cases and controls. Identifying numbers correspond to controls C001–C004 or cases HD001–HD004 as listed in Table 2. The blot was stripped and reprobed for 18S ribosomal RNA as a loading control.

$Hdh^{CAG(150)}$ mice. Diabetes had not previously been detected in the $Hdh^{CAG(150)}$ line and none of the profiled mice exhibited significantly elevated fasting glucose levels. However, abnormal responses were noted in glucose tolerance tests. This unexpected phenotype was investigated further. In our colony of $Hdh^{CAG(150)}$ mice, abnormal glucose homeostasis was detectable by 3 months of age and developed in an age- and genotype-dependent manner (Fig. 5). The homozygous mice were significantly different from the other two genotypes overall and at each individual age. In particular, the homozygous to wild-type difference was significant at 3 months ($P \leq 0.034$), 6 months ($P \leq 0.006$) and 12 months ($P \leq 0.001$). Although consistently higher than the control mice, the heterozygous to wild-type difference was not significant overall ($P \leq 0.15$) or at any age.

The HD signature is present in muscle from $Hdh^{CAG(150)}$ knock-in mice

As expected, there were significantly fewer differentially expressed probe sets in the $Hdh^{CAG(150)}$ mice than in the R6/2 mice. Only 175 probe sets met the $P < 0.001$ criteria (Supplementary Material and http://HDBase.org). Repeating the use of the one-sided Mann–Whitney test on the 250 top R6/2 increases and decreases yielded permutation-based *P*-values for relatedness between R6/2 and $Hdh^{CAG(150)}$ muscles of $P = 0.02$ for increasing and $P < 0.0001$ for decreasing genes. Thus, the strong and reproducible R6/2 muscle phenotype was discernable in the trends in a small microarray experiment on $Hdh^{CAG(150)}$ mice with an extremely subtle phenotype.

DISCUSSION

We have described for the first time skeletal muscle gene expression changes common to mouse and human HD. Our hypothesis that pronounced phenotypes in R6/2 mice can illuminate subtle human phenotypes is supported by the results of this study. Although there are clearly R6/2-specific changes in muscle gene expression, it is apparent that there is a predictable core of changes related to metabolic and myofibrillar

Table 4. Quantitative RT–PCR confirmation of human gene expression changes.

	Symbol	log FC	*P* value
Repressed in HD			
actinin, alpha 3	*ACTN3*	**−2.3**	**0.009**
adenylate kinase 1	*AK1*	**−0.8**	**0.010**
calsequestrin 1	*CASQ1*	**−1.0**	**0.003**
lactate dehydrogenase A	*LDHA*	**−1.4**	**0.001**
phosphofructokinase, muscle	*PFKM*	0.1	0.434
troponin C2, fast	*TNNC2*	**−1.2**	**0.019**
troponin I, skeletal, fast	*TNNI2*	**−0.8**	**0.011**
triosephosphate isomerase	*TPI1*	**−0.3**	0.271
Induced in HD			
actinin, alpha 2	*ACTN2*	0.0	0.492
calsequestrin 2	*CASQ2*	**0.3**	0.234
heat shock 90kDa protein 1, alpha	*HSPCA*	**0.4**	0.165
lactate dehydrogenase B	*LDHB*	**1.3**	**0.032**
lipoprotein lipase	*LPL*	**0.6**	**0.050**

All genes were normalized to troponin C 1 message levels within a sample. The log2 of the fold change, HD/controls, as determined by RT–PCR is shown. Numbers in bold type indicate agreement with microarray data with respect to direction of change or $P \leq 0.05$.

adaptations in both mouse and human HD. Furthermore, within this core phenotype, R6/2 mice are more severely affected than $Hdh^{CAG(150)}$ knock-in mice, and older R6/2 mice are more severely affected than younger R6/2 mice. This progression with overall disease suggests that muscle gene expression or some other biochemical property of muscle may be a useful biomarker for human clinical trials. However, testing this idea will require further study in order to define the most informative set of gene expression changes and measure their longitudinal evolution in human HD. These studies are underway. The skeletal muscle phenotype also raises the possibility that common pathologic mechanisms may be at work in neurons and muscle cells. In our view, it most is likely that the HD muscle phenotype represents a response to multiple factors including endocrine-system changes, muscle-specific polyglutamine effects and aberrant signaling from the central nervous system (CNS). The implications of these mechanisms for HD muscle gene expression as a biomarker and their relationship to current views of neuropathogenic mechanisms shall be discussed.

Muscle fibers are classified as type I (slow-twitch), type IIA (fast-twitch oxidative) and type IIB fibers (fast-twitch glycolytic) (20,21). The proportion of slow and fast fibers within each specific muscle varies, and these ratios respond to a variety of stimuli. A simple interpretation of our data is that mutant huntingtin directly or indirectly triggers in mice and humans, a progressive loss of fast glycolytic fibers and concomitant gain in slow fibers. This is consistent with the conclusion of a recent examination of R6/2 muscle atrophy using histochemical differential staining methods (9). However, the initial examination of R6/2 skeletal muscle, while noting a pronounced reduction in muscle fiber diameter, a result confirmed by Ribchester *et al.* (9), found no immunohistochemical evidence of fiber-type conversion (8). We have not been able to reliably distinguish R6/2 and wild-type skeletal muscle using ATPase staining and antibodies to fast and slow myosin heavy chains (data not shown).

Immunohistochemical methods may not be specific or sensitive enough to detect classic fiber-type switching in R6/2 muscle and the short window between onset and death in R6/2 mice may not be sufficient for large amounts of myofibrillar protein turnover. Alternatively, HD may push fibers toward intermediate phenotypes promiscuously expressing both fast and slow type genes.

Muscle responds to endocrine signals such as growth hormone, insulin, thyroid hormone and sex hormones (20,21). It is well known that the R6/2 and N171 mouse HD models develop diabetes (12–14,29) and there are reports of high diabetes rates in human HD (30). Our observation of impaired glucose homeostasis in $Hdh^{CAG(150)}$ mice provides additional evidence for some type of pancreatic dysfunction associated with HD. More extensive endocrine involvement in HD has not been described but this is a plausible explanation for the wasting so often seen late in the disease. Muscle wasting in HD is usually attributed to increased uncontrolled movement. However, studies have shown that patients who do not yet exhibit chorea already have significantly lower body mass indices (BMI) than age- and sex-matched controls (31). Wasting also seems to occur even while patients receive adequate nutrition (1,32). Perhaps significantly, HD patients with higher BMI live longer than leaner patients (33). Each of these observations suggests that some type of body-wide metabolic imbalance develops as HD progresses.

With respect to metabolic adaptations specifically in skeletal muscle, the HD phenotype has much in common with the fasting-induced muscle gene expression program. However, fasting and diabetes cannot fully explain the HD gene expression pattern. In particular, our study indicates HD causes greater repression of glycolytic enzyme gene expression than does fasting. Further, distinguishing the HD muscle phenotype from metabolic adaptation, a study on muscle gene expression changes caused by diabetes, fasting and cachexia specifically noted an absence of fast and slow myofibrillar protein shifts (17). Our data indicates that decreased expression of genes associated with fast muscle fibers is an early component of the HD muscle phenotype in both mouse and human HD.

Much of the HD muscle phenotype may be muscle-autonomous responses to polyglutamine-related toxicity. The induction of genes encoding chaperones, heat shock proteins and proteasomal-subunits are most simply explained as muscle-cell autonomous events intended to cope with misfolded or aggregated polyglutamine. Transcriptional dysfunction has received much attention in the HD field (2,34,35) and this could be another muscle-intrinsic component of the HD phenotype. In experiments designed to see whether mutant huntingtin protein affects the ability of the MyoD transcription factor (36) to drive myogenesis, no difference was detected between fibroblasts derived from HD patients and controls (S. Tapscott, unpublished data). This result does not necessarily eliminate interference with transcription factors involved in maintenance of the terminally differentiated muscle state as a contributing factor behind the HD phenotype. Recently, mice with functional deletion of the transcription factor PGC-1 were shown to develop clasping, hyperactivity and striatal lesions similar to R6/2 mice (37). Interestingly, prior to that study, PGC-1 was best known for regulating

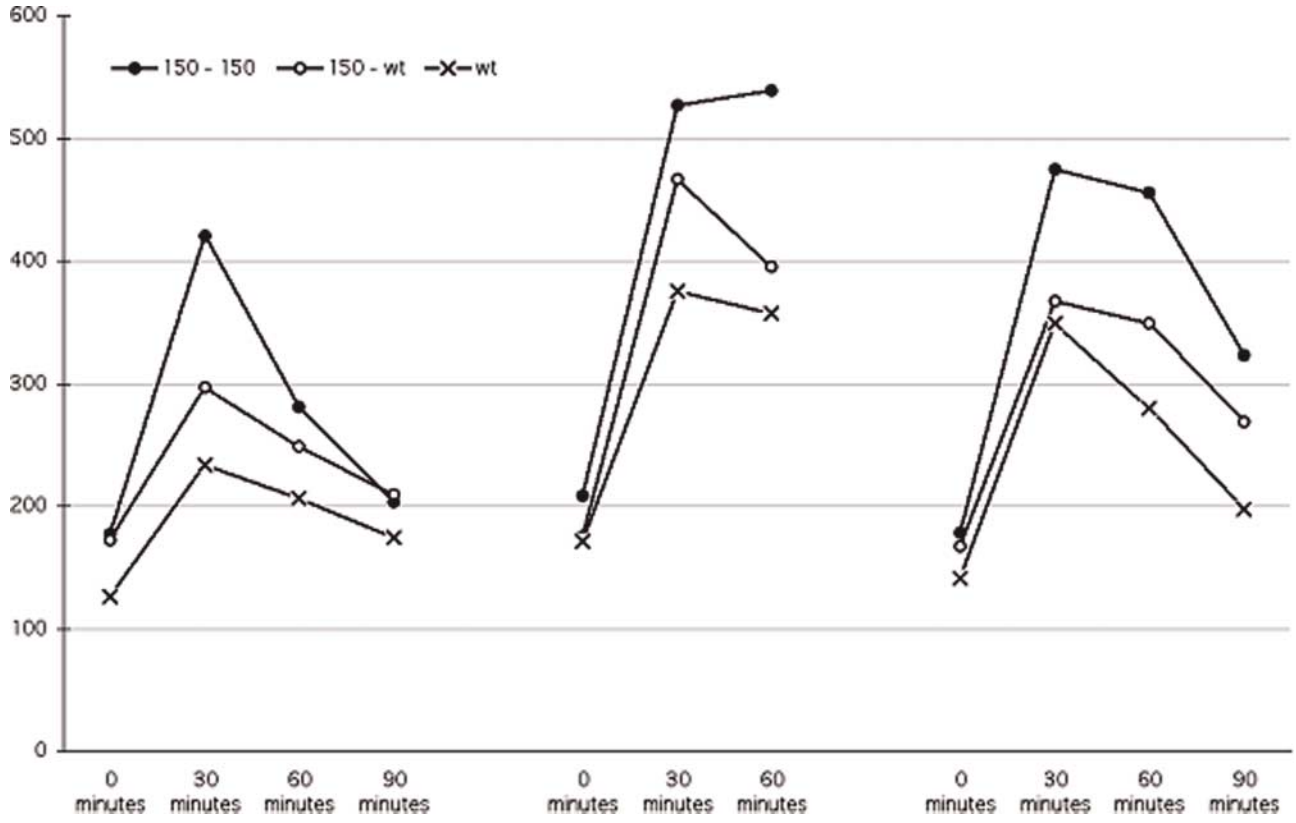

Figure 5. Glucose tolerance tests in $Hdh^{CAG(150)}$ mice. Blood sugar levels were determined after a 6 h fast ($t = 0$), then at 30 min intervals following intraperitoneal glucose injection. Mean glucose levels (mg/dl) for each genotype at each age and time post-challenge are plotted.

gene expression pathways central to mitochondrial oxidative metabolism, fiber-type switching in skeletal muscle and the fasting response in liver (38). To our knowledge, the gene expression profile of those mice has not been made but it might be informative to compare their profile with that of the R6/2 mice.

Factors known to trigger the transition from fast to slow-twitch muscle fibers include aging, hypothyroidism, chronic low frequency stimulation, endurance training and depletion of the high energy phosphate compounds phosphocreatine and ATP (20,21,39). The HD gene expression profile is apparent when age-/sex-matched controls are used; therefore, aging and gender effects seem unlikely explanations for the HD muscle phenotype. The wasting seen in HD patients and R6/2 mice would also seem to mitigate against a simple hypothyroid condition. The other two mechanisms for fast-to-slow transitions, energy depletion and chronic stimulation, are obviously relevant to HD.

Fiber type shifts caused by depleting muscle cells of high-energy compounds are interesting in light of evidence suggesting that metabolic dysfunction in HD-affected neurons leads to excitotoxic mechanisms of neural death and dysfunction (40,41). Inhibitors of oxidative-phosphorylation are used as chemical models of HD (42) and there is evidence that mutant huntingtin directly affects mitochondrial function (43). Defects in mitochondrial energy metabolism have been detected in brain and muscle of presymptomatic HD and DRPLA patients (44–46). It is worthy of note that the defect of ATP production by mitochondrial oxidative phosphorylation in skeletal muscle in HD patients correlates with the length of the CAG repeat, i.e. the longer the repeat, the more severe the mitochondrial defect (44). Finally, dietary supplements that may augment energy stores, such as creatine and co-enzymeQ, appear to have positive effects in mouse models of HD (47–49).

An alternative, but not mutually exclusive hypothesis to explain the HD muscle phenotype is aberrant input from the CNS. Classic studies have shown that muscle fibers will switch type depending on whether they are ectopically innervated by a slow or a fast motor neuron (50). Other studies have shown that chronic low frequency stimulation of muscle contraction causes a fast fiber to become a slow fiber (51,52). Thus, fiber-type switching is due to electrical activity rather than factors released by the motor neuron (20,21,50–53). The definitive symptom of adult HD is chorea. It is possible that increased motor neuron activity, leading to chorea in the human HD and tremors in the mice, triggers adaptations in muscle. The combination of metabolic and myofibrillar adaptations induced by HD are the opposite of changes caused by denervation or inactivity (20,21). Thus paradoxically, as the disease becomes more debilitating, it appears the gene expression profile of HD skeletal muscle becomes more similar to that of muscle undergoing endurance training.

A biomarker has been defined as an objectively measured indicator of a normal biological process, pathogenic process or response to therapeutic intervention (54). All biomarkers must undergo rigorous scrutiny before they are used as surrogate clinical endpoints for therapeutic trials. They must correlate with disease, demonstrate prognostic value and finally provide mechanistic understanding. However, because there is a highly specific diagnostic test for HD, it may not be necessary that muscle gene expression changes, or any HD biomarker for that matter, be specific to HD in order to be of clinical utility. Obviously, the most severe and disturbing symptoms of HD can be traced to effects in the central nervous system. In this study, we have demonstrated that skeletal muscle, an accessible peripheral tissue, is also affected in HD. Importantly, these effects are seen in mouse models of HD and human HD patients. Our studies rule out secondary effects, such as diabetes, weight loss and adipose infiltration, as trivial causes of the muscle phenotype. The muscle phenotype is clearly progressive in R6/2 mice and further studies are underway to correlate muscle gene expression with human HD. To that extent subclinical manifestations of HD in non-CNS tissues, such as skeletal muscle gene expression, can be correlated with disease, they will allow us to objectively measure HD progression in future therapeutic trials. To the extent dysfunction in these tissues shares features with neuronal dysfunction, these phenotypes will also provide new insights into disease mechanisms, which may in turn lead to potential therapies.

MATERIALS AND METHODS

Human studies

Biopsies of vastus lateralis muscle were obtained after informed consent and with the approval of the Royal Free Hospital Trust Ethics Committee and the Institutional Review Boards of the University of Washington and the Fred Hutchinson Cancer Research Center. Biopsies were obtained under local anesthesia and immediately frozen in dry ice or liquid nitrogen. Eight human HD samples and seven unaffected control samples were hybridized to Affymetrix HG_U133A arrays. The HG_U133A arrays contain 22 283 probe sets.

Animal studies

Animal studies were conducted in accordance with the NIH Guide for the Care and Use of Laboratory Animals and with approval of the Fred Hutchinson Cancer Research Center Institutional Animal Care and Use Committee. Glucose tolerance tests were performed on mice that had been fasted for 4 h. After weighing and establishing baseline blood-glucose levels, mice were injected intraperitoneally with 1.5 g glucose/kg body weight. Tail-vein blood samples were collected at half-hour intervals after injection. Glucose levels were measured with a One Touch Lite glucose monitoring system (Lifescan Inc., Milpitas, CA, USA). To outline the scope of diabetes involvement in the muscle phenotype, R6/2 mice were implanted with a single Linbit insulin pellet (LinShin Canada, Inc., Scarborough, Ontario, Canada) at 8 weeks of age. Cohorts of wild-type and R6/2 mice were implanted with placebo pellets in parallel. These mice were sacrificed 3 weeks later to generate gene expression profiles of 11-week-old mice. To define the fasting response, an additional cohort of wild-type mice was placed on a fast 48 h prior to sacrifice. All fasted animals had free access to water. Three R6/2 and three wild-type controls were used for the 15-week profiles. Three homozygous $Hdh^{CAG(150)}$ and three wild-type littermate controls were used to make profiles of 6-month-old $Hdh^{CAG(150)}$ mice. Mouse samples were hybridized to Affymetrix U74Av2 arrays containing 12 488 probe sets.

RNA isolation, cRNA preparation and array hybridization

Human and mouse quadriceps muscle samples were homogenized in TRIZOL (Invitrogen, Carlsbad, CA, USA) using a rotor-stator. Total RNA was isolated according to the manufacturer's protocol. Residual phenol and salts were removed by passage of the total RNA over an RNeasy column (Qiagen, Valencia, CA, USA). Five micrograms of total RNA was used for cRNA synthesis per one-cycle amplification instructions (Affymetrix, Santa Clara, CA, USA). Fifteen micrograms of fragmented cRNA from each sample was used for array hybridization.

Statistical analysis

Primary analysis of microarray data was performed using Bioconductor, an open source and open development software project that provides tools for the analysis and comprehension of genomic data (18,24–27). RMA from the Bioconductor package 'Affy' was used to normalize the arrays. The Bioconductor package 'LIMMA' was used for model fitting, calculation of fold-change, moderated *t*-statistics and corresponding *P*-values. Secondary analysis was performed using Affymetrix MAS 5.0 software.

To define the R6/2 HD muscle phenotype, probe sets were ranked by the absolute value of the sum of the Bioconductor moderated *t*-statistics from the independent 11-week R6/2 + placebo-to-control and the 15-week R6/2-to-control comparisons. This rank-ordered list was used for gene ontology searches and in cross comparisons between R6/2, human, and $Hdh^{CAG(150)}$ HD.

To map genes across species and array platforms, we used two slightly different bioinformatic data clean-up methods. For the Mann–Whitney tests, U74Av2 and HG-U133A probe sets were sorted by their Unigene identifiers and average signals. In the case of redundant probe sets, the probe set with the highest mean signal was kept and the others were discarded. This turned the 12 488 mouse probes into 9287 genes and turned the 22 283 human probes into 14 065 genes. The 9287 genes were considered when performing the R6/2 and $Hdh^{CAG(150)}$ Mann–Whitney test. Using Affymetix information (http://www.affymetrix.com/support/technical/byproduct.affx?cat=exparrays), 6398 orthologous genes were identified and considered for the R/2 and human Mann–Whitney test.

For Figure 3, HG-U133A orthologs of the U74Av2 probe sets were again identified using Affymetix information and sequentially assigned ranks per the mouse list. If a mouse probe set mapped to several human probe sets, the signals of

the redundant human probe sets were averaged. This established one-to-one correspondence between the mouse and human lists. The mouse direction of change was imposed on the human gene by multiplying the human data by -1 if the gene decreased in R6/2 muscle. Finally, for each number g, we computed the average of the normalized first g genes for each individual human sample, and a P-value using a regular one-sided t-test on the two groups of sample averages. A one-sided test was appropriate as we were also testing that the mouse direction of change occurred in the human data. Specifically, the gth P-value was calculated from:

$$t_g = \frac{\bar{X}_{\mathrm{HD,g}} - \bar{X}_{\mathrm{WT,g}}}{\sigma_{\mathrm{p,g}}\sqrt{\left(\frac{1}{n_{\mathrm{HD}}} + \frac{1}{n_{\mathrm{WT}}}\right)}}$$

where $\bar{X}_{\mathrm{HD(WT),g}}$ is the mean of the HD or WT signal averaged over the top g genes, $n_{\mathrm{HD(WT)}}$ the number of HD or WT samples and $\sigma_{\mathrm{p,g}}$ the pooled estimate of standard deviation based on the top g genes. To estimate the frequency that an observed minimum P-value might occur within the first 100 genes by chance, we performed 10 000 randomizations of the data. The direction of change, assigned rank and probe set-signals were randomized simultaneously.

The significance of $Hdh^{CAG(150)}$ genotype on glucose levels was analyzed using a linear mixed effects model (55), treating each mouse as a random effect and genotype, time (categorical), age and weight as fixed effects. Sample sizes for wild-type, heterozygous and homozygous mice were, respectively, 4, 5 and 8 at 3 months; 4, 4 and 5 at 6 months and 4, 10 and 11 at 12 months.

Semiquantitative PCR

Three micrograms of human muscle total RNA was used as template for oligo-dT primed cDNA using Superscript II reverse transcriptase as per the manufacture's recommendations (Invitrogen). Reactions were diluted to 1 ml with distilled water to make stock cDNA solutions. Semiquantitative PCR was set up using SYBR-Green Master Mix (Applied Biosystems, Foster City, CA, USA). About 2.5 μl of cDNA and specific primers at 0.3 μM final concentration were used in 25 μl reactions. All primer pairs were designed to span at least one intron. Cycling was carried out on the Applied Biosystems 7000 Sequence Detector. Samples were held at 95°C for 10 min, then cycled 40 times from 95°C for 20 s to 55°C for 30 s. SYBR-Green I intensity was analyzed using ABI SDS 7000 v.1.0 software. Reactions were performed in triplicate. All detection-threshold cycle-count values were normalized to *troponin C1* levels. *Troponin C1* was chosen because the mouse and human microarray data indicated that its expression was relatively unaffected by HD or fasting. Genes such as *actin, beta-tubulin* and *GAPDH* that are often used as normalization controls were unsuitable in our case because they were identified as HD-affected genes in mouse or human muscle by microarray. Relative gene expression levels were calculated using the ΔCT method (56). P-values were calculated using a standard one-tailed t-test as we were interested in a predetermined direction of change. PCR primer sequences can be found in Supplementary Material.

SUPPLEMENTARY MATERIAL

Supplementary Material is available at HMG Online.

ACKNOWLEDGEMENTS

A.D.S. thanks Fred Schachat for explaining nuances of muscle fiber types and providing important technical advice, Mark Aronszajn for computer assistance, Jeff Delrow and the staff of the FHCRC array facility, Sally Ditzler for her expert help with all the animal studies, Chin Hsing Lin for assistance with *HdhCAG(150)* mice and Miriam Rosenberg for technical assistance. A.D.S. and J.M.O. were supported by the Cure HD Initiative of the Hereditary Disease Foundation, the High Q Foundation and NIH grant RO1 NS42157. C.L.K. and A.K.A. were supported in part by NIH grant CA 074841. S.J.T. is a United Kingdom Department of Health National Clinician Scientist. C.T. was a Wellcome Training Fellow.

Conflict of Interest statement. None declared.

REFERENCES

1. Hayden, M.R. and Kremer, B. (2001) In Scriver, C., Beaudet, A., Sly, W. and Valle, D. (eds), *The Metabolic and Molecular Basis of Inherited Disease.* 8th edn. McGraw-Hill, New York, USA. pp. 5677–5701.
2. Ross, C.A. (2002) Polygutamine pathogenesis: emergence of unifying mechanisms for Huntington's disease and related disorders. *Neuron*, **35**, 819–822.
3. Mangiarini, L., Sathasivam, K., Seller, M., Cozens, B., Harper, A., Hetherington, C., Lawton, M., Trottier, Y., Lehrach, H., Davies, S.W. and Bates, G.P. (1996) Exon 1 of the *HD* gene with an expanded CAG repeat is sufficient to cause a progressive neurological phenotype in transgenic mice. *Cell*, **87**, 493–506.
4. Menalled, L.B. and Chesselet, M.F. (2002) Mouse models of Huntington's disease. *Trends Pharmacol. Sci.*, **23**, 32–39.
5. Lin, C.H., Tallaksen-Greene, S., Chien, W.M., Cearley, J.A., Jackson, W.S., Crouse, A.B., Ren, S., Li, X.J., Albin, R.L. and Detloff, P.J. (2001) Neurological abnormalities in a knock-in mouse model of Huntington's disease. *Hum. Mol. Genet.*, **10**, 137–144.
6. Huntington Study Group (1996) The unified Huntington's disease rating scale: reliability and consistency. *Mov. Disord.*, **11**, 136–142.
7. Marder, K., Zhao, H., Myers, R.H., Cudkowicz, M., Kayson, E., Kieburtz, K., Orme, C., Paulsen, J., Penney, J.B., Jr, Siemers, E. *et al.* (2000) Rate of functional decline in Huntington's disease. Huntington Study Group. *Neurology*, **54**, 452–458.
8. Sathasivam, K., Hobbs, C., Turmaine, M., Mangiarini, L., Mahal, A., Bertaux, F., Wanker, E.E., Doherty, P., Davies, S.W. and Bates, G.P. (1999) Formation of polyglutamine inclusions in non-CNS tissue. *Hum. Mol. Genet.*, **8**, 813–822.
9. Ribchester, R.R., Thomson, D., Wood, N.I., Hinks, T., Gillingwater, T.H., Wishart, T.M., Court, F.A., and Morton, A.J. (2004) Progressive abnormalities in skeletal muscle and neuromuscular junctions of transgenic mice expressing the Huntington's disease mutation. *Eur. J. Neurosci.*, **20**, 3092–3114.
10. Luthi-Carter, R., Hanson, S.A., Strand, A.D., Bergstrom, D.A., Chun, W., Peters, N.L., Woods, A.M., Chan, E.Y.W., Kooperberg, C., Young, A.B. *et al.* (2002) Dysregulation of gene expression in the R6/2 model of polyglutamine disease: parallel changes in muscle and brain. *Hum. Mol. Genet.*, **11**, 1911–1926.
11. Hockly, E., Woodman, B., Mahal, A., Lewis, C.M. and Bates, G., (2003) Standardization and statistical approaches to therapeutic trials in the R6/2 mouse. *Brain Res. Bull.* **61**, 469–479.
12. Hurlbert, M.S., Zhou, W., Wasmeier, C., Kaddis, F.G., Hutton, J.C., and Freed, C.R. (1999) Mice transgenic for an expanded CAG repeat in the Huntington's disease gene develop diabetes. *Diabetes*, **48**, 649–651.

13. Andreassen, O.A., Dedeoglu, A., Stanojevic, V., Hughes, D.B., Browne, S.E., Leech, C.A., Ferrante, R.J., Habener, J.F., Beal, M.F. and Thomas, M.K. (2002) Huntington's disease of the endocrine pancreas. Insulin deficiency and diabetes mellitus due to impaired insulin gene expression. *Neurobiol. Dis.*, **11**, 410–424.
14. Bjorkqvist, M., Fex, M., Renstrom, E., Wierup, N., Petersen, A., Gil, J., Bacos, K., Popovic, N., Li, J.Y., Sundler, F., Brundin, P. and Mulder, H. (2005) The R6/2 transgenic mouse model of Huntington's disease develops diabetes due to deficient {beta}-cell mass and exocytosis. *Hum. Mol. Genet.*, **14**, 565–574.
15. Sreekumar, R., Halvatsiotis, P., Schimke, J.C. and Nair, K.S. (2002) Gene expression profile of skeletal muscle of type 2 diabetes and the effect of insulin treatment. *Diabetes*, **51**, 1913–1920.
16. Jagoe, R.T., Lecker, S.H., Gomes, M. and Goldberg, A.L. (2002) Patterns of gene expression in atrophying skeletal muscles: response to food deprivation. *FASEB J.*, **16**, 1697–1712.
17. Lecker, S.H., Jagoe, R.T., Gilbert, A., Gomes, M., Baracos, V., Bailey, J., Price, S.R., Mitch, W.E. and Goldberg, A.L. (2004) Multiple types of skeletal muscle atrophy involve a common program of changes in gene expression. *FASEB J.*, **18**, 39–51.
18. Smyth, G.K., (2004) Linear models and empirical Bayes methods for assessing differential expression in microarray experiments. *Stat. Appl. Genet. Mol. Biol.*, **3**, Article 1.
19. Dennis, G. Jr., Sherman, B.T., Hosack, D.A., Yang, J., Baseler, M.W., Lane, H.C. and Lempicki, R.A. (2003) DAVID: database for annotation, visualization, and integrated discovery. *Genome Biol.*, **4**, P3. (http://apps1.niaid.nih.gov/david/upload.asp).
20. Fluck, M. and Hoppeler, H. (2003) Molecular basis of skeletal muscle plasticity–from gene to form and function. *Rev. Physiol. Biochem. Pharmacol.*, **146**, 159–216.
21. Berchtold, M.W., Brinkmeier, H. and Muntener, M. (2000) Calcium ion in skeletal muscle: its crucial role for muscle function, plasticity, and disease. *Physiol. Rev.*, **80**, 1215–1265.
22. Van Hall, G. (2000) Lactate as a fuel for mitochondrial respiration. *Acta Physiol. Scand.*, **168**, 643–656.
23. Mills, M., Yang, N., Weinberger, R., Vander Woude, D.L., Beggs, A.H., Easteal, S. and North, K. (2001) Differential expression of the actin-binding proteins, alpha-actinin-2 and -3, in different species: implications for the evolution of functional redundancy. *Hum. Mol. Genet.*, **10**, 1335–1346.
24. Campbell, W.G., Gordon, S.E., Carlson, C.J., Pattison, J.S., Hamilton, M.T. and Booth, F.W. (2001) Differential global gene expression in red and white skeletal muscle. *Am. J. Physiol. Cell Physiol.*, **280**, C763–C768.
25. Gentleman, R.C., Carey, V.J., Bates, D.M., Bolstad, B., Dettling, M., Dudoit, S., Ellis, B., Gautier, L., Ge, Y., Gentry, J. *et al.* (2004) Bioconductor: open software development for computational biology and bioinformatics. *Genome Biol.*, **5**, R80.
26. Ihaka, R. and Gentleman, R., (1996) R: A language for data analysis and graphics. *J. Comput. Graph. Stat.*, **5**, 299–314.
27. Irizarry, R., Gautier, L. and Cope, L. (2003) An R package for oligonucleotide array statistical analysis. In Parmigiani, G., Garrett, E.S., Irizarry, R. and Zeger, S.L. (eds), *The Analysis of Gene Expression Data: Methods and Software.* Springer, New York, NY.
28. Cononver, W.J. (1980) *Practical Nonparametric Statistics*, 2nd edn. John Wiley and Sons, Inc., New York, NY.
29. Duan, W., Guo, Z., Jiang, H., Ware, M., Li, X.J. and Mattson, M.P. (2003) Dietary restriction normalizes glucose metabolism and BDNF levels, slows disease progression, and increases survival in huntingtin mutant mice. *Proc. Natl Acad. Sci. USA*, **100**, 2911–2916.
30. Farrer, L.A. (1985) Diabetes mellitus in Huntington disease. *Clin. Genet.*, **27**, 62–77.
31. Djousse, L., Knowlton, B., Cupples, L.A., Marder, K., Shoulson, I. and Myers, R.H. (2002) Weight loss in early stage of Huntington's disease. *Neurology* **59**, 1325–1330.
32. Morales, L.M., Estevez, J., Suarez, H., Villalobos, R., Chacin de Bonilla, L. and Bonilla, E. (1989) Nutritional evaluation of Huntington disease patients. *Am. J. Clin. Nutr.*, **50**, 145–150.
33. Myers, R.H., Sax, D.S., Koroshetz, W.J., Mastromauro, C., Cupples, L.A., Kiely, D.K., Pettengill, F.K. and Bird, E.D. (1991) Factors associated with slow progression in Huntington's disease. *Arch. Neurol.*, **48**, 800–804.
34. Sugars, K.L. and Rubinsztein, D.C. (2003) Transcriptional abnormalities in Huntington disease. *Trends Genet.*, **19**, 233–238.
35. Li, S.H. and Li, X.J. (2004) Huntingtin–protein interactions and the pathogenesis of Huntington's disease. *Trends Genet.*, **20**, 146–154.
36. Tapscott, S.J., Davis, R.L., Thayer, M.J., Cheng, P.F., Weintraub, H. and Lassar, A.B. (1988) MyoD1: a nuclear phosphoprotein requiring a Myc homology region to convert fibroblasts to myoblasts. *Science*, **242**, 405–411.
37. Lin, J., Wu, P.H., Tarr, P.T., Lindenberg, K.S., St-Pierre, J., Zhang, C.Y., Mootha, V.K., Jager, S., Vianna, C.R., Reznick, R.M. *et al.* (2004) Defects in adaptive energy metabolism with CNS-linked hyperactivity in PGC-1alpha null mice. *Cell*, **119**, 121–135.
38. Puigserver P. and Spiegelman, B.M. (2003) Peroxisome proliferator-activated receptor-gamma coactivator 1 alpha (PGC-1 alpha): transcriptional coactivator and metabolic regulator. *Endocr. Rev.*, **24**, 78–90.
39. Ohira, Y., Kawano, F., Roy, R.R., and Edgerton, V.R. (2003) Metabolic modulation of muscle fiber properties unrelated to mechanical stimuli. *Jpn. J. Physiol.*, **53**, 389–400.
40. Schapira, A.H. (1998) Mitochondrial dysfunction in neurodegenerative disorders. *Biochem. Biophys. Acta*, **1366**, 225–233.
41. Browne, S.E. and Beal, M.F. (2004) The energetics of Huntington's disease. *Neurochem. Res.*, **29**, 531–546.
42. Brouillet, E., Conde, F., Beal, M.F. and Hantraye, P. (1999) Replicating Huntington's disease phenotype in experimental animals. *Prog. Neurobiol.*, **59**, 427–468.
43. Panov, A.V., Gutekunst, C.A., Leavitt, B.R., Hayden, M.R., Burke, J.R., Strittmatter, W.J. and Greenamyre, J.T. (2002) Early mitochondrial calcium defects in Huntington's disease are a direct effect of polyglutamines. *Nat. Neurosci.*, **5**, 731–736.
44. Lodi, R., Schapira, A.H., Manners, D., Styles, P., Wood, N.W., Taylor, D.J. and Warner, T.T. (2000) Abnormal *in vivo* skeletal muscle energy metabolism in Huntington's disease and dentatorubropallidoluysian atrophy. *Ann. Neurol.*, **48**, 72–76.
45. Gu, M., Gash, M.T., Mann, V.M., Javoy-Agid, F., Cooper, J.M. and Schapira, A.H. (1996) Mitochondrial defect in Huntington's disease caudate nucleus. *Ann. Neurol.*, **39**, 385–389.
46. Tabrizi, S.J., Cleeter, M.W., Xuereb, J., Taanman, J.W., Cooper, J.M. and Schapira, A.H. (1999) Biochemical abnormalities and excitotoxicity in Huntington's disease brain. *Ann. Neurol.*, **45**, 25–32.
47. Andreassen, O.A., Dedeoglu, A., Ferrante, R.J., Jenkins, B.G., Ferrante, K.L., Thomas, M., Friedlich, A., Browne, S.E., Schilling, G., Borchelt, D.R. *et al.* (2001) Creatine increases survival and delays motor symptoms in a transgenic animal model of Huntington's disease. *Neurobiol. Dis.*, **8**, 479–491.
48. Ferrante, R.J., Andreassen, O.A., Dedeoglu, A., Ferrante, K.L., Jenkins, B.G., Hersch, S.M. and Beal, M.F. (2002) Therapeutic effects of coenzyme Q10 and remacemide in transgenic mouse models of Huntington's disease. *J. Neurosci.*, **22**, 1592–1599.
49. Schilling, G., Coonfield, M.L., Ross, C.A., and Borchelt, D.R. (2001) Coenzyme Q10 and remacemide hydrochloride ameliorate motor deficits in a Huntington's disease transgenic mouse model. *Neurosci. Lett.*, **315**, 149–153.
50. Buller, A.J., Eccles, J.C. and Eccles, R.M. (1960) Interactions between motoneurones and muscles in respect of the characteristic speeds of their responses. *J. Physiol.*, **150**, 417–439.
51. Eken, T. and Gundersen, K. (1988) Electrical stimulation resembling normal motor-unit activity: effects on denervated fast and slow rat muscles *J. Physiol.*, **402**, 651–669.
52. Windisch, A., Gundersen, K., Szabolcs, M.J., Gruber, H. and Lomo, T. (1998) Fast to slow transformation of denervated and electrically stimulated rat muscle. *J. Physiol.*, **510**, 623–632.
53. Buonanno, A. and Fields, R.D. (1999) Gene regulation by patterned electrical activity during neural and skeletal muscle development. *Curr. Opin. Neurobiol.*, **9**, 110–120.
54. Biomarkers Definitions Working Group. (2001) Biomarkers and surrogate endpoints: preferred definitions and conceptual framework. *Clin. Pharmacol. Ther.*, **69**, 89–95.
55. Laird, N.M. and Ware, J.H. (1982) Random-effects models for longitudinal data. *Biometrics*, **38**, 963–974.
56. Livak, K.J. and Schmittgen, T.D. (2001) Analysis of relative gene expression data using real-time quantitative PCR and the 2(-Delta Delta C(T)) method. *Methods*, **25**, 402–408.